DE GRUYTER Sci Eng Compos Mater 2016; 23(4): 407–412

Wenfeng Li, Suping Li* and Xiangchong Zhong

Comparing the influence of different kinds of zirconia on properties and microstructure of Al_2O_3 ceramics

Abstract: This paper compared the influence of fused zirconia-corundum (AZ40), monoclinic zirconia (m-ZrO_2), and 3 mol% yttria-stabilized zirconia (3Y-ZrO_2) on physical properties at room temperature, hot modulus of rupture, and thermal shock resistance of Al_2O_3 ceramics, and their relationships with microstructure changes were investigated. It was found that m-ZrO_2 or 3Y-ZrO_2 addition promoted the process of sintering densification and enhanced the room temperature strength and the hot modulus of rupture of Al_2O_3 ceramics, and the effect of the latter was more distinct, while those of the sample with AZ40 addition decreased. In addition, the three kinds of ZrO_2 were beneficial to improving the thermal shock resistance of Al_2O_3 ceramics. All these changes had close relationships with the changes of corresponding microstructure characteristics (including distribution of particles, degree of contact between crystals, grain boundary solid solution, microcrack density) and phase composition.

Keywords: Al_2O_3 ceramics; hot modulus of rupture; microstructure; phase composition; thermal shock resistance; ZrO_2.

DOI 10.1515/secm-2014-0232
Received July 19, 2014; accepted September 28, 2014; previously published online December 22, 2014

1 Introduction

Alumina (Al_2O_3) is considered as one of the most interesting ceramic candidates regarding its high melting point and excellent mechanical properties, such as high hardness, good chemical and thermal stability [1]. However, the application of Al_2O_3 ceramics is limited by their inherent brittle nature, which often leads to catastrophic failure, especially under impact and tensile stress conditions [2, 3]. One of the methods to improve this property is by introducing a moderate quantity of ZrO_2 into Al_2O_3 ceramics; the mechanism of this process is based on the stress-induced phase transition from tetragonal zirconia (t-ZrO_2) to monoclinic zirconia (m-ZrO_2) [4–8]. Thus, the dispersion of ZrO_2 in Al_2O_3 matrix results in a Al_2O_3/ZrO_2 composite with higher hardness, elastic modulus, high temperature mechanical properties, and heat-shock property, and it is mainly used as cutting tools, bearings, high-temperature gas burner, knee replacement prostheses, and so on [9, 10].

Fused zirconia-corundum is one of the important ZrO_2-containing materials, which contains a typical eutectic microstructure. Composites with a stoichiometry close to the eutectic point of around 40–42 wt.% ZrO_2 are found to exhibit excellent thermal stability and mechanical properties [11–13]. Some reports have pointed out that when the ZrO_2 contains 3 mol.% Y_2O_3, the partially stabilized ZrO_2 possesses excellent strength and fracture toughness [14, 15].

In this work, fused zirconia-corundum, 3 mol% Y_2O_3 stabilized ZrO_2, and m-ZrO_2 were introduced into Al_2O_3 ceramics. The purpose was to compare the influence of them on physical properties at room temperature, hot modulus of rupture, and thermal shock resistance of Al_2O_3 ceramics, and their relationships with microstructure changes (including distribution of particles, degree of contact between crystals, grain boundary solid solution, microcrack density) and phase composition were discussed.

2 Materials and methods

2.1 Starting materials and sample preparation

The starting materials used in the present work were fused zirconia-corundum with its chemical composition of 59.4% α-Al_2O_3-33.2% m-ZrO_2-7.4% t-ZrO_2 (denoted

***Corresponding author: Suping Li,** School of Materials Science and Engineering, Zhengzhou University, Zhengzhou 450052, China, e-mail: lisupinghtci@gmail.com
Wenfeng Li and Xiangchong Zhong: School of Materials Science and Engineering, Zhengzhou University, Zhengzhou 450052, China

as AZ40, ≤7 μm), 3 mol% yttria-stabilized zirconia with its chemical composition of 76.2% t-ZrO_2-23.8% m-ZrO_2 (marked as 3Y-ZrO_2, ≤7 μm), monoclinic zirconia (ZrO_2 ≥99.0%, ≤7 μm), and white fused corundum (α-Al_2O_3 ≥98.5%, ≤44 μm). The mass ratio of α-Al_2O_3 to ZrO_2 was 85/15, ZrO_2 was introduced into Al_2O_3 ceramics in forms of AZ40, m-ZrO_2, and 3Y-ZrO_2, denoted as Z_1, Z_2 and Z_3, respectively, and the sample without ZrO_2 addition was marked as Z_0. These materials were weighed in terms of this mass ratio and mixed for 1 h in a polyurethane bottle with water and zirconia balls, then pressed at 150 MPa into samples with sizes of 180 mm×15 mm×15 mm and ∅ 36 mm×36 mm, and sintered in air. The thermal profile was a ramp of 7°C/min to 1100°C, 2°C/min to 1200°C, and followed by a ramp of 3°C /min to 1650°C, held for 3 h.

2.2 Sample characterization

Bulk density and apparent porosity were measured using Archimedes' principle in water medium. Permanent linear change was examined by measuring the change in length of samples before and after firing. The modulus of rupture at room temperature and at 1400°C were determined by the standard three-point bending method. Cold crushing strength was measured using a hydraulic press machine in accordance with ISO 10059-1:1992. In thermal shock tests, the samples were heated to 1100°C and then quickly quenched in air. After three thermal shock cycles, the residual strength (σ_r) was measured and compared with the original strength (σ_f). Residual strength ratio (σ_r/σ_f) at ΔT=1100°C was a criterion for evaluating thermal shock resistance.

The phase contents were conducted using Philips X-ray diffractometer (XRD) with Cu Ka radiation (λ=1.5406 Å) in the 2θ range of 20–80°C for a period of 3°/min in the step scan mode. Microstructure and composition of samples were investigated by scanning electron microscopy (SEM, JEOL JSM-5610LV) equipped with an energy-dispersive spectrometry (EDS).

3 Results and discussion

3.1 Physical properties at room temperature

The permanent linear change, apparent porosity, and bulk density of samples are listed in Table 1, showing that the addition of m-ZrO_2 or 3Y-ZrO_2 can promote the process of sintering densification, while AZ40 addition results in a volume expansion and reduces the densification of Al_2O_3 ceramics.

Table 1 Permanent linear change, apparent porosity and bulk density of samples.

Sample	Z_0	Z_1	Z_2	Z_3
Permanent linear change (%)	-3.91	+3.80	-4.90	-6.85
Apparent porosity (%)	28.27	40.89	25.60	22.29
Bulk density (g/cm³)	2.95	2.40	3.08	3.23

Figure 1 shows the microstructures of samples Z_0, Z_2, and Z_3. In contrast to samples Z_2 and Z_3, the SEM photograph of the Al_2O_3 sample shown in Figure 1A has a microstructure with coarse grains and large gaps, indicating a weak interface between crystals. For the sample with m-ZrO_2 or 3Y-ZrO_2 addition (see Figure 1B and C, respectively), the presence of the two distinct phases, Al_2O_3 (darker phase) and ZrO_2 (brighter phase), can clearly be observed. It is clear that ZrO_2 particles are homogeneously distributed in corundum skeleton structure inhibiting abnormal grain growth of Al_2O_3 and leading the dense structure.

The micrograph of the AZ40 starting material shown in Figure 2A is a typical eutectic microstructure, which is made up of faceted colonies with a size of around 10–15 μm that consist of ordered ZrO_2 phases within the Al_2O_3 matrix. When it is introduced into Al_2O_3 ceramics and sintered at 1650°C for 3 h, the eutectic microstructure no longer exists, which is substituted by the microstructure that consists of coarse ZrO_2 particles within the Al_2O_3 matrix, as shown in Figure 2B. The grown ZrO_2 particles cannot be suppressed by Al_2O_3 matrix, t-phase has transformed spontaneously to m-phase during the cooling process. This is supported by the XRD pattern shown in Figure 4A; it can be seen that there is few t-ZrO_2 in the sample. The phase transformation of these grown t-ZrO_2 particles are accompanied by the volume expansion and crack formation, as shown in Figure 2C, which leads to a decrease in the density of Al_2O_3 ceramics.

Cold crushing strength and modulus of rupture of samples are shown in Figure 3. As Figure 3 shows, m-ZrO_2 or 3Y-ZrO_2 addition is beneficial to improving the room temperature strength of Al_2O_3 ceramics, and the effect of the latter is more distinct, while those of the sample with AZ40 addition decrease.

The improvement of the room temperature strength of samples is primarily attributed to the stress-induced phase transformation toughening and the enhancement of density. Through XRD analysis on the surfaces of samples, as shown in Figure 4, monoclinic peaks at the $(11\bar{1})$ and (111) planes and tetragonal peak at the (111) plane of ZrO_2

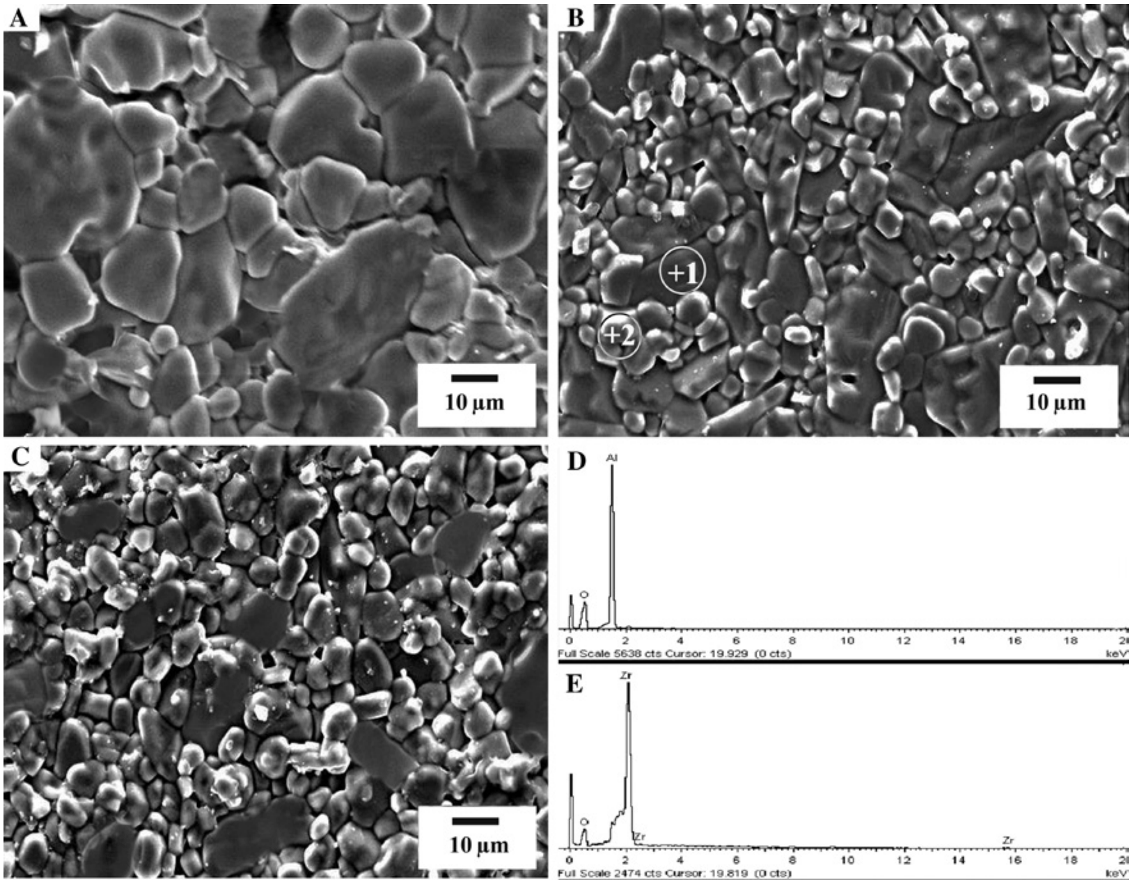

Figure 1 SEM photographs of samples (A) Z_0, (B) Z_2, (C) Z_3, (D) and (E) EDS spectrum of scanned sites 1 and 2 in (B), respectively.

are detected; the amount of t-ZrO_2 in samples is evaluated using Eq. (1) and Eq. (2) below [16]:

$$X_m = \frac{I_m(111)+I_m(11\bar{1})}{I_m(111)+I_m(11\bar{1})+I_t(111)} \quad (1)$$

$$X_t = 1\text{-}X_m \quad (2)$$

Here, X is the relative content in the sample, I is the absolute intensity, and the subscripts m and t refer to the monoclinic and the tetragonal phase, respectively.

For the sample with 3Y-ZrO_2 addition, the amount of t-ZrO_2 is calculated and found to be 12% and 5% on the fracture face before and after sample failure, respectively, indicating that a portion of t-ZrO_2 has transformed into m-phase during the modulus of rupture test, the crack propagation can be prevented by compressive stress due to this stress-induced phase transformation. In addition, the sample with 3Y-ZrO_2 addition has a dense structure. All these are important strengthening effects contributing to improvement of the room temperature strength of

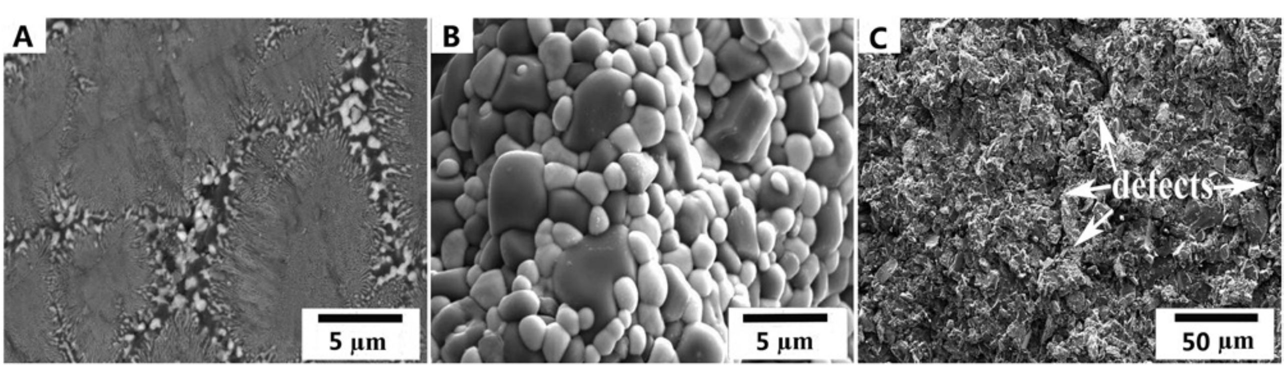

Figure 2 SEM photographs of (A) AZ40 starting material, (B) AZ40 after 3 h at 1650°C, (C) the sample with AZ40 addition.

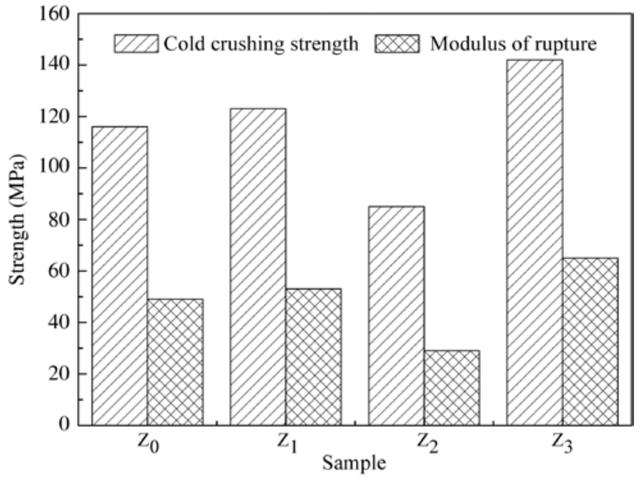

Figure 3 Cold crushing strength and modulus of rupture of samples.

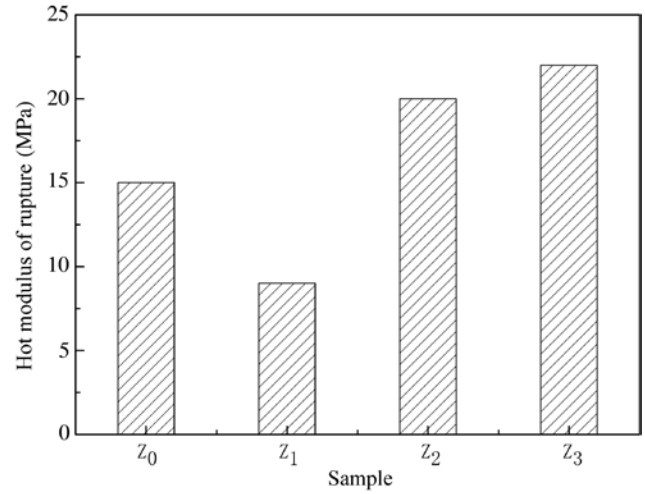

Figure 5 Hot modulus of rupture of samples at 1400°C.

Al_2O_3 ceramics. But there is only a negligible amount of t-ZrO_2 in the sample with m-ZrO_2 addition; thus, the slight enhancement of its room temperature strength can be explained by the dense structure. As shown in the marked area by the arrows in Figure 2C, there is obvious defects in the sample with AZ40 addition, which lead to a decrease in room temperature strength of Al_2O_3 ceramics.

3.2 Hot modulus of rupture

Figure 5 shows the hot modulus of rupture of samples at 1400°C. It can be seen that the addition of m-ZrO_2 or 3Y-ZrO_2 can improve the hot modulus of rupture of Al_2O_3 ceramics, the values of them are 20 MPa and 22 MPa, respectively, while that of the sample with AZ40 addition decreases to 9 MPa.

Some reports have pointed out that the principal factors influencing high temperature mechanical properties are the crystal effect and the glass effect [17, 18]. In this work, there is practically no glass phase in the samples; the controlling factor is the crystal effect (degree and mode of contact or bonding between crystals).

Figure 6 shows the fracture surfaces of samples Z_1, Z_2, and Z_3 after hot modulus of rupture test. In comparison with sample Z_1, there are fewer gaps and pores between crystals in the sample with m-ZrO_2 or 3Y-ZrO_2 addition (see Figure 6C and D, respectively), indicating a strong interface between crystals. Moreover, the study on the bonding between Al_2O_3-ZrO_2 by SEM and EDS shown in Figure 7 and Table 2 indicates that at the Al_2O_3-ZrO_2 interface, there is interdiffusion at grain boundaries between the two phases. All these are important strengthening effects contributing to improvement of the hot modulus of rupture of Al_2O_3 ceramics. The SEM photograph of the sample with AZ40 addition shown in Figure 6A has a microstructure with large gaps and defects, the AZ40 particles grow during heat treatment to form larger particles with a diameter ranging from 8 μm to 20 μm due to the martensitic transformation of ZrO_2, and even some ZrO_2 particles drop out from the Al_2O_3 matrix in AZ40 particles (see Figure 6B). These defects result in a decrease in the hot modulus of rupture of Al_2O_3 ceramics.

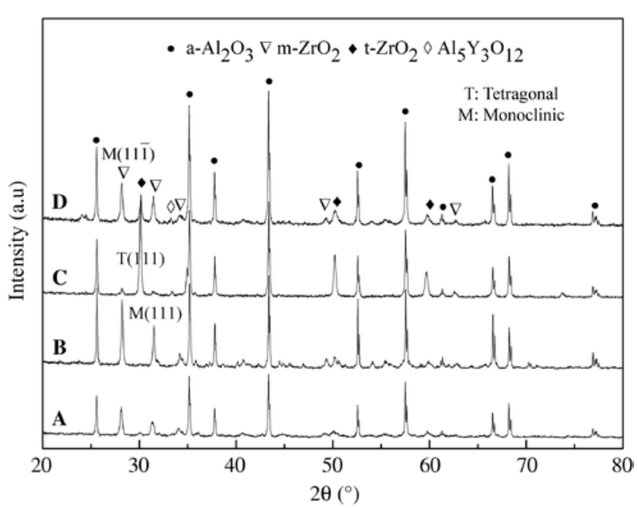

Figure 4 XRD patterns of the surfaces of samples (A) Z_1, (B) Z_2, (C) Z_3, (D) Z_3 after the modulus of rupture test.

3.3 Thermal shock resistance

The results of the thermal shock resistance of the samples are shown in Figure 8. As can be seen in Figure 8, the

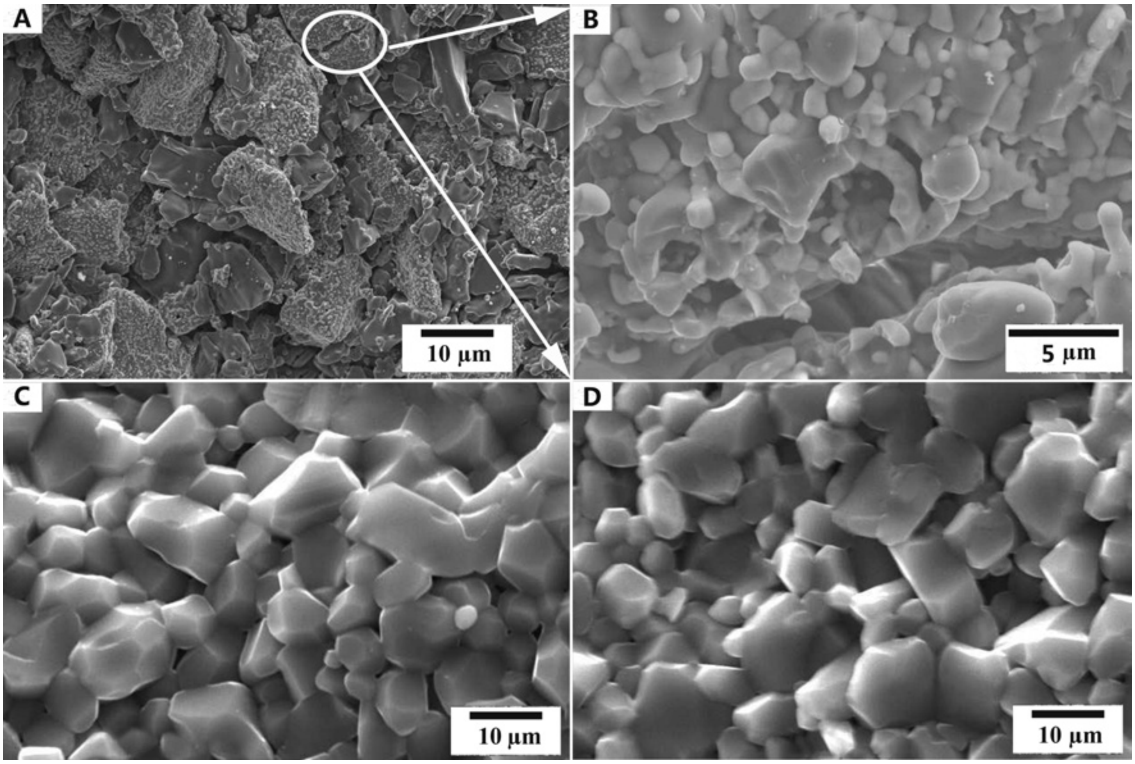

Figure 6 Fracture surfaces of samples (A) Z_1, (B) the magnification of the marked area in (A), (C) Z_2, and (D) Z_3.

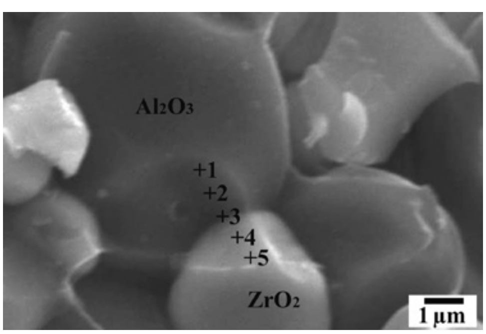

Figure 7 SEM photograph showing bonding between zirconia and corundum (the sample Z_3).

three kinds of ZrO_2 are beneficial to improving the thermal shock resistance of Al_2O_3 ceramics, the residual strength ratios of samples Z_1, Z_2, and Z_3 are 62%, 68%, and 71%, respectively, and the maximum residual strength of 44 MPa is achieved from the sample Z_3.

Table 2 Composition of scanned sites of corundum and zirconia particles in Figure 7 by EDS.

Scanned site	1	2	3	4	5
Al_2O_3 (%)	98.07	93.67	58.53	6.72	3.82
ZrO_2 (%)	1.93	6.33	41.36	93.06	95.93
Y_2O_3 (%)	–	–	0.11	0.22	0.25

In order to further evaluate the thermal shock resistance behavior, the microstructures of samples Z_1, Z_2, and Z_3 after thermal shock tests are examined, as shown in Figure 9. Some microcracks are observed on the surfaces of all the samples due to the spontaneous transformation of ZrO_2, which can relax the stress concentration to enhance the thermal shock resistance of Al_2O_3 ceramics. In addition, for the sample with 3Y-ZrO_2 addition, t-ZrO_2 can prevent crack propagation by compressive stress due to

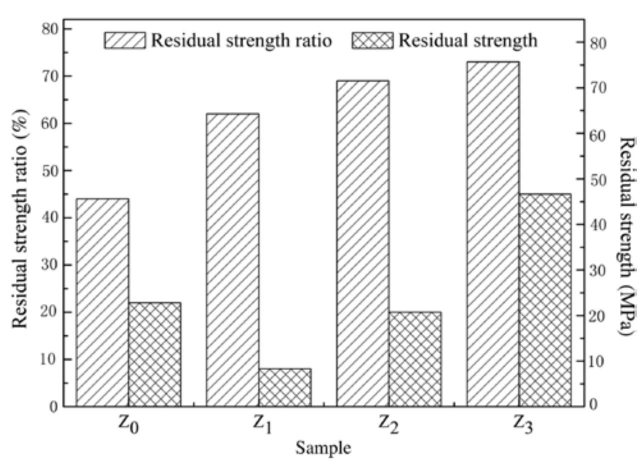

Figure 8 Residual strength ratio and residual strength of samples (ΔT=1100°C).

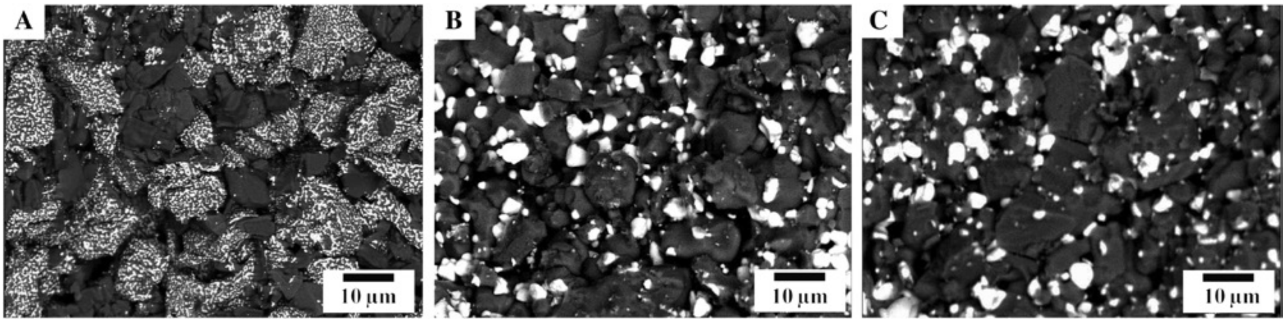

Figure 9 SEM photographs of samples (A) Z_1, (B) Z_2, (C) Z_3 after thermal shock tests at ΔT=1100°C.

the stress-induced phase transformation, which is beneficial to enhancing the residual strength of Al_2O_3 ceramics.

4 Conclusions

This paper compared the influence of AZ40, m-ZrO_2, and 3Y-ZrO_2 on the properties and microstructure of Al_2O_3 ceramics. The main results obtained were summarized as follows:

1. m-ZrO_2 or 3Y-ZrO_2 addition promoted the process of sintering densification of Al_2O_3 ceramics due to the distributions of ZrO_2, which inhibited abnormal grain growth of Al_2O_3 and led the dense structure, while AZ40 addition resulted in a volume expansion because of the phase transformation of the grown ZrO_2 particles.
2. m-ZrO_2 or 3Y-ZrO_2 addition was beneficial to improving the room temperature strength of Al_2O_3 ceramics, and the effect of the latter was more distinct because of the stress-induced phase transformation toughening, while that of the sample with AZ40 addition decreased due to the defects in the sample.
3. The hot modulus of rupture of Al_2O_3 ceramics was enhanced by adding m-ZrO_2 or 3Y-ZrO_2, which was attributed to the enhancement of density and the interdiffusion at grain boundaries between $A1_2O_3$ and ZrO_2 crystals, but that of the sample with AZ40 addition decreased.
4. The three kinds of ZrO_2 were beneficial to improving the thermal shock resistance of Al_2O_3 ceramics because of the microcracks, induced by the martensitic transformation of ZrO_2, which could relax stress concentrations and lead to toughening.

Acknowledgments: This work was supported by the Henan Research Program of Application Foundation and Advanced Technology (No. 122300410244), and the authors would like to express their appreciation to the High Temperature Ceramics Institute of Zhengzhou University for providing the necessary facilities during the experimentation and tests and also thank Dr. Huishi Guo, Dr. Zhen Ren, and Prof. Xinhong Liu for the helpful discussions and encouragements, and Prof. Enxia Xu and Prof. Quanli Jia for the assistance with the experiment.

References

[1] Rao PG, Iwasa M, Tanaka T, Kondoh I, Inoue T. *Scr. Mater.* 2003, 48, 437–441.
[2] Wahsh MMS, Khattab RM, Awaad M. *Mater. Des.* 2012, 41, 31–36.
[3] Maiti K, Sil A. *Ceram. Int.* 2011, 37, 11–21.
[4] Smuk B, Szutkowska M, Walter J. *J. Mater. Process. Technol.* 2003, 133, 195–198.
[5] Tuan WH, Chen RZ, Wang TC, Cheng CH, Kuo PS. *J. Eur. Ceram. Soc.* 2002, 22, 2827–2833.
[6] Jang HM, Cho SM, Kim KT. *J. Mater. Sci.* 1996, 31, 5083–5092.
[7] Zhang XF, Li YC. *Mater. Des.* 2010, 31, 1945–1952.
[8] Rittidech A, Somrit R, Tunkasiri T. *Ceram. Int.* 2013, 39, 433–436.
[9] Zu YF, Chen GQ, Fu XS, Luo KG, Wang CG, Song SP, Zhou WL. *Ceram. Int.* 2014, 40, 3989–3993.
[10] Ma WM, Wen L, Guan RG, Sun XD, Li XK. *Mater. Sci. Eng. A* 2008, 477, 100–106.
[11] Chen GQ, Fu XS, Luo JT, Zu YF, Zhou WL. *J. Eur. Ceram. Soc.* 2012, 32, 4195–4204.
[12] Zheng YT, Li HB, Zhou T, Zhao J, Yang P. *J. Alloys Compd.* 2013, 551, 475–480.
[13] Suffner J, Sieger H, Hahn H, Dosta S, Cano IG, Guilemany JM, Klimczyk P, Jaworska L. *Mater. Sci. Eng. A* 2009, 506, 180–186.
[14] Chen GQ, Zu YF, Luo JT, Fu XS, Zhou WL. *Mater. Sci. Eng. A* 2012, 554, 6–11.
[15] Kuo CW, Shen YH, Yen FL, Cheng HZ, Hung IM, Wen SB, Wang MC, Stack M. *Ceram. Int.* 2014, 40, 3243–3251.
[16] Xu YG, Huang ZH, Liu YG, Fang MH, Yin L, Guan M. *Solid State Sci.* 2012, 14, 730–734.
[17] Zhong XC. *Sci. Press* 1984, 13, 254–261.
[18] Zhong XC, Zhao HL. *Bull. Acers* 2000, 79, 59–61.